Evol Ecol
DOI 10.1007/s10682-016-9826-7

ORIGINAL PAPER

Flower reshaping in the transition to hummingbird pollination in Loasaceae subfam. Loasoideae despite absence of corolla tubes or spurs

Marina M. Strelin[1] · Santiago Benitez-Vieyra[1] · Markus Ackermann[2,3] · Andrea A. Cocucci[1]

Received: 8 October 2015 / Accepted: 14 March 2016

Abstract Many angiosperm lineages present transitions from bee to hummingbird pollination. The flower design in most of these lineages includes either corolla tubes or nectar spurs, structures that commonly experienced an elongation with the acquisition of hummingbird pollination. It is proposed that this increases the fit between the bird head and flower structures, and isolates or partially blocks bees from the interaction. But can this transition occur if the ancestral flower design lacks tubes or spurs? Here we focus on the transition from bee to hummingbird pollination in the Loasaceae subfamily Loasoideae. Loasoideae flowers have radial corollas with separated petals; therefore, they do not display corolla tubes nor nectar spurs. These flowers also present a whorl of nectar scales and staminodes, unique to the subfamily, which is involved in flower–pollinator fit and in nectar harvesting. To explore flower shape adaptation to hummingbird pollination, we tested for correspondence between pollinators and flower shape in Loasoideae. In order to achieve this, we first compared the evolutionary history of flower phenotype and pollination mode, and then used stochastic character mapping and geometric-morphometric variables in a comparison of alternative evolutionary models. The results of our study suggest that the transition from bee to bird pollination was accompanied by changes in the shape of the staminodial complex, along with the evolution of relatively closed corollas. Moreover, while bird pollination seems to be the end point in the evolution of

Electronic supplementary material The online version of this article (doi:10.1007/s10682-016-9826-7) contains supplementary material, which is available to authorized users.

✉ Marina M. Strelin
marina.strelin85@gmail.com

[1] Laboratorio de Ecología Evolutiva y Biología Floral, Instituto Multidisciplinario de Biología Vegetal (Consejo Nacional de Investigaciones Científicas y Técnicas–Universidad Nacional de Córdoba), Casilla de Correo 495, X5000ZAA Córdoba, Argentina

[2] Present Address: Institut für Integrierte Naturwissenschaften – Biologie, Universität Koblenz-Landau, Universitätsstr. 1, 56070 Koblenz, Germany

[3] Nees Institut für Biodiversität der Pflanzen, Rheinische Friedrich-Wilhelms-Universität, Meckenheimer Allee 170, 53115 Bonn, Germany

pollination syndromes in many angiosperm lineages, rodent pollinated flowers probably evolved from ancestral bird pollinated flowers in Loasoideae. Our findings suggest that the evolution of bird pollinated flowers from ancestral bee pollinated flowers does not require the presence of corolla tubes or spurs, and can take place as long as the flower design includes structures participating in flower–pollinator fit.

Keywords Loasoideae · Pollinator selection · Hummingbird pollination · Bee pollination · Flower shape

Introduction

The evolutionary versatility of flower traits can be frequently related to different pollination and reproductive modes, and is considered one of the most important drivers of angiosperm speciation and diversification (Van der Niet and Johnson 2012). Flowering plants differ markedly in morphological traits involved in flower–pollinator fit, and in physiological traits such as nectar composition, flower colour and fragrance, all of which are involved in pollinator reward and attraction. Certain suites of these traits are commonly associated with specific, functional groups of pollinators (e.g. bats, bees, birds) constituting pollination syndromes (Fenster et al. 2004; Thomson and Wilson 2008; Rosas-Guerrero et al. 2014).

Some evolutionary transitions between pollination syndromes are more frequently reported than others, being the transition from bee to bird pollination the prevailing one (van der Niet and Johnson 2012; Rosas-Guerrero et al. 2014). This transition involve changes in flower morphology (narrower and longer corollas), in flower color, (redder flowers in bird pollinated species, in some cases), and in nectar characteristics (lower sugar concentration and higher nectar volumes) (reviewed in Thomson and Wilson 2008).

Studies addressing macro-evolutionary patterns in plant lineages that experienced transitions from bee to bird pollination, e.g. *Penstemon* (Wilson et al. 2004), *Ruellia* (Acanthaceae) (Tripp and Manos 2008) and *Salvia* (Benitez-Vieyra et al. 2014), support the theory of a correlated evolution between pollinators and flower traits. These lineages share a similar flower design consisting of tubular corollas, which restrict access to the nectar contained at their bottom. As a response to bird pollination, these lineages have generally experienced evolutionary lengthening of corolla tubes, increasing the fit between the bird head and the fertile flower organs (Thomson and Wilson 2008). This either diminishes the efficiency of bee pollination (Ashworth et al. 2015) or even totally excludes bees from the interaction (Thomson and Wilson 2008), as was experimentally demonstrated for *Penstemon* by Castellanos et al. (2004). *Aquilegia* presents an exception to this flower design since it displays a petal appendage, the nectar spur, which is involved in flower–pollinator morphological fit, and whose length increased during transitions from bee to bird pollination (Whittall and Hodges 2007). Previous studies suggest that in lineages with transitions from bee to bird pollination, bird pollination is generally the end point in the evolution of pollination syndromes (reviewed in Barrett 2013), even though reversals or transitions to other pollination modes have also been reported, e.g. reversals to bee-pollination in *Ruellia* (Tripp and Manos 2008) and transitions from hummingbird to moth-pollination in *Aquilegia* (Whittall and Hodges 2007).

Loasaceae subfam. Loasoideae is a monophyletic and mostly Neotropical angiosperm subfamily of approximately 200 species, with its centre of diversity in the Central Andes. While bee pollination appears to be the ancestral condition in this subfamily, hummingbird pollination emerged at least twice during its evolution (Ackermann and Weigend 2006): two of the most diverse Loasoideae genera, *Caiophora* C.Presl and *Nasa* Weigend, include hummingbird pollinated species (Weigend and Gottschling 2006; Ackermann and Weigend 2006). The genus *Caiophora* also includes a single rodent pollinated species, *Caiophora coronata* (Cocucci and Sérsic 1998). Loasoideae flowers are actinomorphic, they present divided corollas and pouch-shaped petals which protect the antepetalous stamens (Fig. 1). The flowers bear in their centre five antesepalous staminodial complexes, which are unique to this subfamily, each derived from five staminodes. The three outer ones are united into a nectar scale and bear the two inner, free staminodes (Fig. 1) (Brown and Kaul 1981; Hufford 2003). This complex functions as a nectar reservoir and is proposed to mediate flower–pollinator fit (Weigend 2004; Weigend et al. 2010) (Fig. 1).

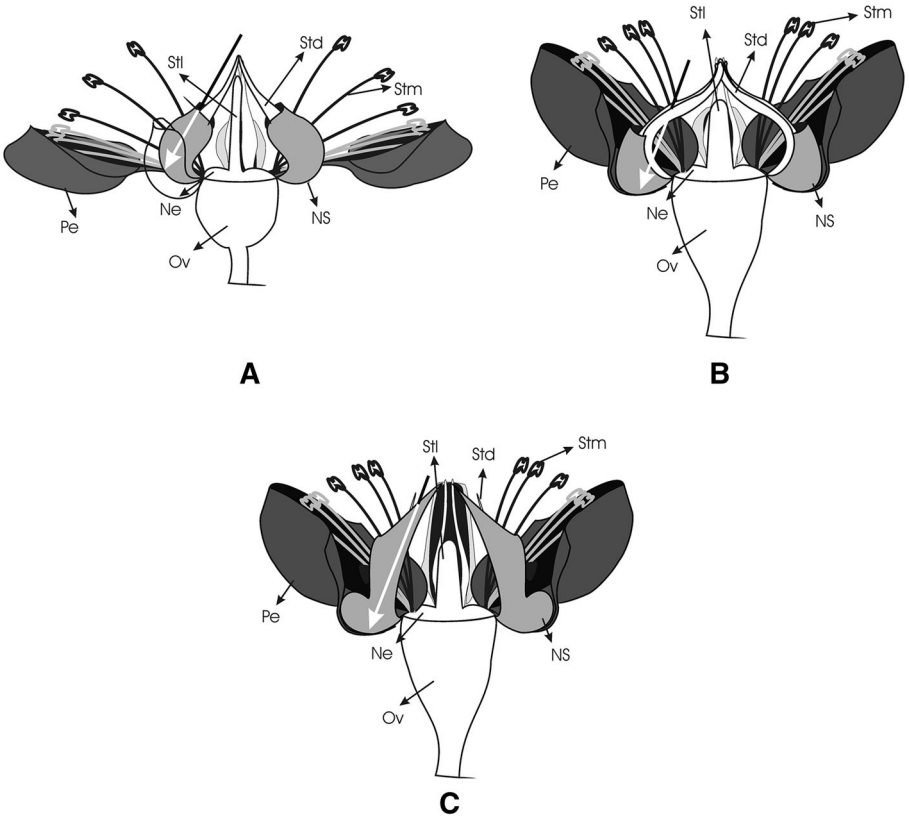

Fig. 1 Schematic representation of flower shape in Loasoideae and expected pollinator behaviour in **a** "Tilt-revolver" and **b**, **c** "Funnel-revolver" flowers of **b** *Caiophora* and **c** *Nasa*. The *arrows* indicate **a** the position in which bees insert their proboscises to access nectar (the nectar scale moves outwards), and **b**, **c** the direction in which the staminodes guide the hummingbirds beak towards nectar. Flower structures are indicated. *Pe* petal, *Stl* style, *Std* staminode, *Stm* stamen, *NS* nectar scale, *Ne* nectary, *Ov* ovary

Previous works (Ackermann and Weigend 2006; Weigend and Gottschling 2006) suggest that the bee pollination syndrome is ancestral in Loasoideae and that switches to hummingbird pollination have taken place repeatedly in this subfamily. Nevertheless, these studies did not consider the association between the pollination mode and floral morphology in a phylogenetic context, i.e. they neither inquired about ancestral pollination strategies nor tested whether flower morphology evolved in response to pollinator-mediated selection. The aim of the present study is to answer whether flower shape responded to selection by different pollinators (bees, birds and rodents) in Loasoideae, an angiosperm lineage which lacks corolla tubes; and, in the case it did so, to determine the optimal shapes for each pollination mode in this lineage.

After obtaining a phylogeny of Loasoideae, we first reconstructed the evolutionary history of flower shape in this subfamily, following the discrete classification of Ackermann and Weigend (2006) and Weigend and Gottschling (2006). Although these authors proposed alternative flower shapes to represent adaptations to bee and to hummingbird pollination in Loasoideae, this has not been formally tested yet. We examined this proposal using the superposition of evolutionary histories of flower phenotype (including flower shape) and pollinator groups. To directly test for this superposition we also did a correlation analysis. Then, we used geometric morphometric variables to quantitatively represent the shape of the corolla and the staminodial complex in order to evaluate whether the shape of these structures evolved towards different adaptive optima in Loasoideae, corresponding to different pollinator groups.

Materials and methods

"Tilt-revolver" and "funnel-revolver" flowers in Loasoideae

Weigend and Gottschling (2006) separated flower phenotype of Loasoideae in two discrete categories, based on flower shape and colouration. "Tilt-revolver" flowers (TRF) have spreading to reflexed, white to yellow petals and brightly coloured nectar scales, which contrast with the petals and tightly enclose the nectar (Fig. 1a). "Funnel-revolver" flowers (FRF) have half-erect to erect, orange to red petals and nectar scales not contrasting with the petals and hidden inside the corolla. Nectar is easily accessible to pollinators in FRF (Fig. 1b, c). Based on what is known about the pollination mechanism of these two flower phenotypes, TRF are proposed to be adapted to bee pollination, while FRF to hummingbird pollination (Weigend and Gottschling 2006; Ackermann and Weigend 2006). Bees visiting TRF have to hold onto the flower in an inverted position (the staminodial complex at the centre of the flower provides a foothold to the visiting bees) and slide their proboscis between the scale and the two protruding staminodes (which function as a guide to the nectar). The two staminodes block the nectar scale entrance, and while the pollinator slides its proboscis into the scale to access nectar, the scale moves outwards activating the movement of mature stamens (resting inside the pouch-like petals) towards the centre of the flower (Fig. 1a), where anthers place pollen on the abdomen of visiting bees (Weigend et al. 2010). Contrastingly, the nectar scales in FRF are relatively open, allowing access to nectar without manipulation. The staminodial complex guides the beak of visiting hummingbirds to the basal nectar reservoir (Weigend 2004). In *Caiophora*, this guidance is accomplished by the two remarkably elongated and protruding tips of the staminodes (Weigend, personal communication) (Fig. 1b) and in *Nasa* by the widened neck of the

nectar scale (Fig. 1c) (Weigend 2004). The mature stamens are located in a loose bundle in the centre of the flower and dust the hummingbird's head/beak (Weigend and Gottschling 2006). The relatively closed corolla of FRF presumably promotes the fit between the hummingbird head/beak and the fertile structures of the flower, as in other angiosperm lineages with hummingbird pollination (reviewed in Thomson and Wilson 2008).

Phylogeny

To carry out the analyses in this study, it was necessary to make an estimation of the phylogeny with branch lengths and to reconstruct the ancestral pollination strategies. To construct a phylogeny for Loasoideae, we used two plastid regions, matK and trnL-trnF, taken from the NCBI GenBank database (Table S1). We obtained sequences for 40 species, and we also amplified and sequenced five additional species. PCRs were carried out using the protocol described in Hufford (2005). We aligned the sequences with MAFFT (Katoh and Standley 2013) and verified them by eye using PhyDE (Müller et al. 2010). We made a Bayesian estimation of the phylogeny using BEAST v.1.8.0 (Bouckaert et al. 2014) by applying a single model of molecular evolution to both chloroplast markers, specifying a Yule evolutionary process, and using a strict clock, a GTR + Γ + I substitution model with 4 Gamma categories and non-informative priors for all parameters. We ran four independent Monte Carlo Markov chains (MCMC) with 50 million generations each, sampling each 1000 generations (50 thousand trees were retained per chain). We imported log files from each run into TRACER v. 1.5, in order to examine effective sample sizes and stationarity. We discarded the first 5000 trees as burnin and assembled the 45,000 trees retained per chain into a single file (adding up to a total of 180 thousand trees) using LOG COMBINER v.1.8.0. From these 180 thousand trees, we finally obtained the maximum clade credibility tree and randomly sampled a subset of 1000 trees to account for phylogenetic uncertainty in the subsequent analyses. We pruned these trees to 33 terminal taxa for the stochastic character mappings, and to 17 for the model comparison analysis using quantitative data (see below).

Discrete flower phenotypes and pollinator groups

We used 32 species representing nearly all Loasoideae genera, namely, *Aosa* Weigend, *Blumenbachia* Schrad. *Caiophora* C.Presl, *Loasa* Adans, *Nasa* Weigend, *Presliophytum* (Urb. & Gilg) Weigend, *Scyphanthus* Sweet and *Xylopodia* Weigend (Table S2). We classified these 32 species, based on flower phenotype and flower mechanism, as bearing either TRF or FRF flowers. The classification of species in either TRF or FRF was taken from Ackermann and Weigend (2006) and Weigend and Gottschling (2006) (Table S2) or investigated here, according to floral characteristics. We did not consider pollinator data in the TRF–FRF classification.

We obtained pollinator data from Ackermann and Weigend (2006), Weigend and Gottschling (2006) or from literature (Table S2). For those species not included in previous studies, we performed pollinator observations in the field (see Table S2 for qualitative data and Table S3 for quantitative data). We assigned a pollination mode (hummingbird, bee and rodent pollination) to all species based on these records. Four species have ambiguous pollinator records, i.e. they were reported to be pollinated by hummingbirds and bees: *Caiophora chuquitensis* (Macrocarpa and Heptamera morphotypes), *C. lateritia* and *C. hibiscifolia* (Table S2). These were assigned to a single pollination mode, using a linear discriminant analysis (LDA). In order to avoid circularity, LDA included floral traits that

do not overlap with flower shape and help to define bee and hummingbird pollination syndromes in other plant lineages: nectar concentration and nectar volume (Fenster et al. 2004; Thomson and Wilson 2008). We used Loasoideae species pollinated either by bees or by hummingbirds as the training data set (Appendix S4), based on which we predicted the pollination mode of the three species with ambiguous pollinator records. We performed the LDA with the *lda* function of the R package MASS (Venables and Ripley 2002). While *C. hibiscifolia* and *C. chuquitensis* (Macrocarpa and Heptamera morphotypes) were assigned to the hummingbird pollination group, *C. lateritia* was assigned to the bee pollination group (Appendix S4).

To reconstruct the history of pollination modes and flower phenotype (TRF–FRF) in Loasoideae by accounting for phylogenetic uncertainty and uncertainty in ancestral character states, we conducted stochastic character mappings (Nielsen 2002) using the *make.simmap* function from the R package *phytools* (Revell 2012). We performed 10 stochastic character mappings on each of the 1000 randomly sampled BEAST phylogenetic trees, after pruning them to the 33 terminal taxa with pollinator and flower phenotype data (Table S2). Given a set of phylogenies and discrete character states for extant terminal taxa, this Bayesian method applies a Monte Carlo algorithm to sample the posterior probability distribution of ancestral states on the branches of a phylogeny under a Markov process of evolution. We superimposed the phylogenetic trees and the stochastic character mappings in a single plot using the R packages *phytools* (Revell 2012) and *geiger* (Harmon et al. 2008), and calculated the mode of the number of transitions between pollination modes and between flower phenotypes, using the *describe.simmap* function from the R package *phytools* (Revell 2012). In addition, we performed 1000 stochastic character mapping simulations on the maximum posterior credibility BEAST tree, and plotted the posterior probability of each character state on the corresponding node (Revell 2014), using the *describe.simmap* function from the R package *phytools* (Revell 2012). Character states on the nodes of this tree were then used in the model comparison analysis described in the next section. Furthermore, to check for overlap between the evolutionary history of pollination modes and the evolutionary history of flower morphology, we used the *map.overlap* function of the R package *phytools* (Revell 2012) on the set of 1000 mapped phylogenies mentioned above. This function computes the proportional overlap between two mapped histories on a tree or a set of trees. We used the overall D-statistic (Huelsenbeck et al. 2003), implemented in SIMMAP v. 1.5 (Bollback 2006), to test if the evolutionary association between pollination mode and flower phenotype is higher than expected by chance. We also estimated the correlation state-by-state statistics (d_{ij}), which represent the divergence between the observed and expected association of states i and j. For these analyses, we randomly selected 500 trees from their posterior distribution.

Geometric morphometrics of flower traits and model comparison of evolutionary histories

We measured geometric morphometric variables in a subset of 16 species in order to quantitatively represent the shape of the corolla and the staminodial complex. This subsample comprises species of the genera *Blumenbachia, Caiophora* (including two morphotypes of *Caiophora chuquitensis*, Heptamera and Macrocarpa) and *Loasa* (Table S5). Given that some natural populations of the studied species are either small or difficult to access, sample sizes for some species were reduced and some species were sampled at the Botanical Garden of Bonn University, Germany. We sampled between 6 and 25 individuals from the same population per species, and we collected one flower from each individual.

For *Caiophora carduifolia* and *Loasa tricolor*, sampled at the Botanical Garden, only one individual could be sampled. We photographed the corolla and the staminodial complex in the lateral view with a Leica M420 stereomicroscope (Wetzlar, Germany).

We obtained geometric morphometric variables describing the shape of the corolla and of the staminodial complex in order to accomplish a quantitative description of shape variation. We used the program tpsDig (Rohlf 2009) to plot landmarks on the corolla (Fig. 3a) and on the staminodial complex (Fig. 3b), and applied a Procrustes fit to these landmarks to control for size-related variation and position, using the program MorphoJ (Klingenberg 2011). Variation among the configurations of the obtained Procrustes coordinates, therefore, only represents variation in shape. We then computed principal components (PCs hereafter) of the Procrustes coordinates for the corolla and the staminodial complex, using MorphoJ (Klingenberg 2011). These PCs describe variation in the configuration of Procrustes coordinates, hence the variation in shape. We used those PCs accounting for more than 50 % of the total variance in the analyses described below.

To determine if flower shape in the analysed species responded to pollinator selection, we modelled trait evolution with the R package *ouch* (Butler and King 2004), according to three alternative evolutionary scenarios. To establish if the evolution of each flower trait (retained PC) responded to pollinator selection in Loasoideae, we constructed the following three models for each retained PC separately. First, we modelled trait evolution as a Brownian process (BM model). Under this scenario, the trait only evolved through drift, with phylogenetic distance among terminal taxa being the only factor explaining inter-specific trait variability. This model contained, when applied to a single trait, two parameters: σ^2 representing the stochastic evolutionary rate of the focal trait, and θ_0, representing the state of that trait at the basal node of the phylogeny. Second, we modelled trait evolution according to two different Ornstein–Uhlembeck (OU) processes (Hansen 1997). These models involve the conjoined action of drift and selection in determining inter-specific trait variability. Our second model (OU1 model) consisted of the simplest version of an OU model, according to which the trait evolved towards a single adaptive optimum. This model included four parameters: σ^2, representing the stochastic evolutionary rate of the focal trait; α, representing the intensity of selection (the fraction of trait variation that is explained by stabilizing selection and not by drift); θ, representing an optimal trait value towards which the trait evolved under stabilizing selection; and θ_0, representing the state of the trait at the basal node of the phylogeny. The third model (OU3) was also an OU model, but this time we incorporated three different adaptive optima, θ_b, θ_h, θ_r (for bee, hummingbird and rodent pollination selective regimes). These regimes (i.e. pollination modes obtained as explained in the previous section together with their ancestral state reconstruction) were a priori specified by "painting" the branches of the phylogeny (Butler and King 2004) according to how we hypothesized they affected trait evolution. Ancestral pollination modes were reconstructed using the 1000 stochastic character mappings described in the previous section. The mapped tree was then pruned to the 17 taxa with geometric morphometric data. Confidence intervals of each parameter of the three models defined above were obtained by performing 10,000 parametric bootstraps. These confidence intervals spanned the 2.5 % and the 97.5 % quantiles, considering σ^2 and α to be significant, when the confidence interval did not include zero. To select the best fitting model, we compared the AICc and the SIC values (Akaike indexes corrected for sample size and Schwartz information criterion) of the three models and performed likelihood ratio tests. In a second stage, we estimated and compared the three models defined above on 1000 phylogenies randomly sampled from the posterior distribution of BEAST phylogenetic trees, as a way of integrating over uncertainty in phylogeny. Ancestral state

Fig. 2 Stochastic character mappings of **a**, **b** the pollinator and **c**, **d** the flower phenotype. Pollination strategies and flower phenotype are indicated with *colours*. Pollination strategy: *blue* = bee pollination; *green* = hummingbird pollination; *purple* = rodent pollination; flower phenotype: *red* = TRF; *cyan* = FRF. *Panels A* and *C* show the maximum credibility tree with pie charts on its nodes, indicating the posterior probability of **a** each pollination strategy and **c** each flower phenotype retrieved by 1000 stochastic character mappings. *Panels B* and *D* show the superimposition of 1000 phylogenetic trees, with 10 stochastic character mappings each. (Color figure online)

reconstruction for some nodes can also render uncertain results, i.e. different pollination modes have the same posterior probability on a node, which entails a problem for the specification of the OU model with three adaptive optima. Therefore, we followed two alternative approaches to deal with this source of uncertainty in ancestral reconstruction: on the one hand, we arbitrarily considered bee pollination as the ancestral state of all nodes with uncertainty regarding bee pollination versus hummingbird pollination or bee pollination versus rodent pollination; and we considered hummingbird pollination as the ancestral state of all nodes with uncertainty regarding bird pollination versus rodent pollination. These assumptions about ancestral states are based on evidence that indicates that reversion in pollination syndromes is unlikely to occur because of functional, physiological and developmental aspects of the flower phenotype (Whittall and Hodges 2007; Barrett 2013). On the other hand, we randomly chose between hummingbird pollination and bee pollination, bee pollination and rodent pollination, and hummingbird pollination and rodent pollination, assigning this arbitrary ancestral state to the uncertain node. Both procedures were applied to the comparison of evolutionary models in the 1000 trees sampled from the posterior distribution of phylogenetic trees. However, as they yielded almost identical results, we reported the results assuming that bee pollination (or eventually hummingbird pollination) is the ancestral state in all dubious nodes.

Results

The topology of the maximum credibility tree does not differ, in general terms, from the topology reported by Hufford (2005), where *Caiophora* and *Nasa* clearly conform two monophyletic groups. In addition, the two morphotypes of *C. chuquitensis*, Heptamera and Macrocarpa, belong to two distinctive and well supported clades (Fig. S6).

Four independent transitions from bee to hummingbird pollination can be inferred from the studied Loasoideae taxa (mode = 4 transitions, 95 % credible interval = (2, 4)) (Fig. 2a, b). One took place in the genus *Nasa*, the other three in *Caiophora*. One transition from hummingbird to rodent pollination can also be inferred from the stochastic character mapping (mode = 1 transitions, 95 % credible interval = (1, 1)) (Fig. 2a, b). "Tilt-revolver" flowers (TRF) were reconstructed as ancestral to "Funnel-revolver" flowers (FRF), which evolved four times independently (mode = 4 transitions, 95 % credible interval = (3, 4)) (Fig. 2b, c). Similar to what was found for the pollination mode, these evolutionary transitions occurred in the genera *Nasa* and *Caiophora* (Fig. 2c, d). No reversions from hummingbird to bee pollination and from FRF to TRF were found in the studied Loasoideae species (mode = 0 reversions, 95 % credible interval = (0, 2); mode = 0 reversions, 95 % credible interval = (0, 1), respectively) (Fig. 2). The mean proportion of overlap between the evolutionary histories of the pollination strategy and of the flower phenotype was above 0.9 (mean: 0.919, sd.: ±0.0578). We found significant statistical associations between pollination mode and floral type (overall $D = 0.151$, $P < 0.001$, Table 1).

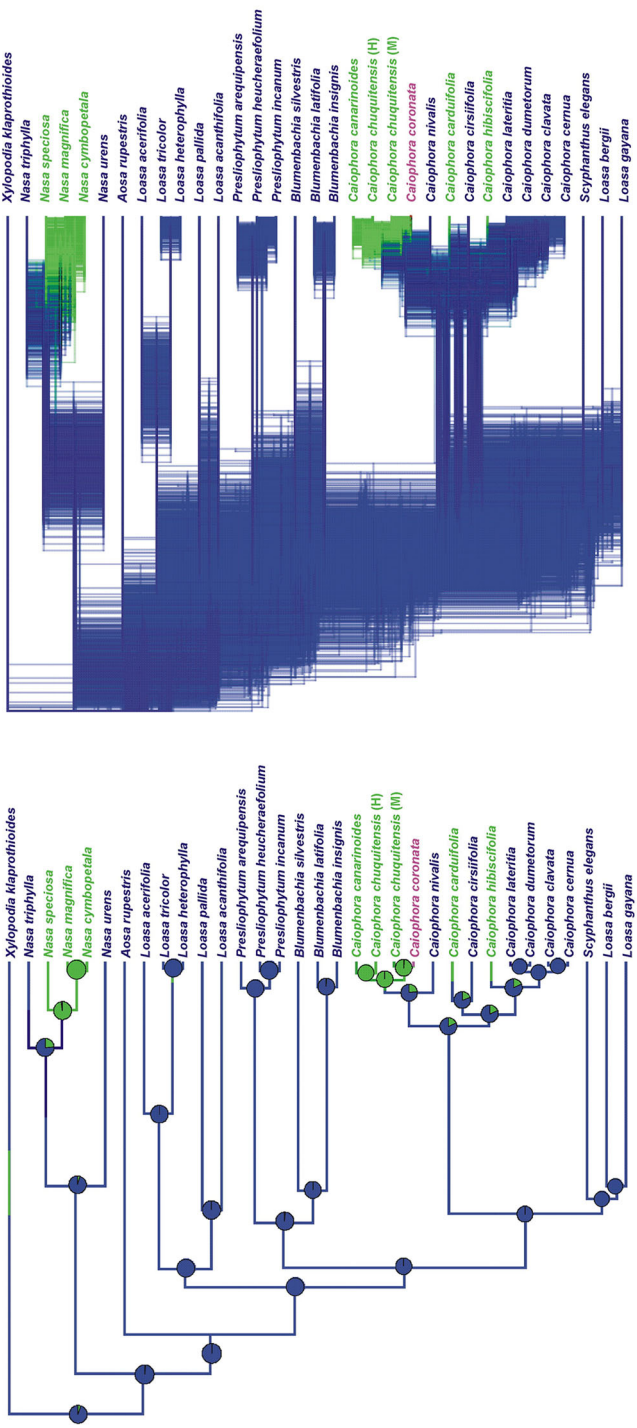
Xylopodia klaprothioides
Nasa triphylla
Nasa speciosa
Nasa magnifica
Nasa cymbopetala
Nasa urens
Aosa rupestris
Loasa aceriifolia
Loasa tricolor
Loasa heterophylla
Loasa pallida
Loasa acanthifolia
Presliophytum arequipensis
Presliophytum heucheraefolium
Presliophytum incanum
Blumenbachia silvestris
Blumenbachia latifolia
Blumenbachia insignis
Caiophora canarinoides
Caiophora chuquitensis (H)
Caiophora chuquitensis (M)
Caiophora coronata
Caiophora nivalis
Caiophora carduifolia
Caiophora cirsiifolia
Caiophora hibiscifolia
Caiophora lateritia
Caiophora dumetorum
Caiophora clavata
Caiophora cernua
Scyphanthus elegans
Loasa bergii
Loasa gayana
A
B

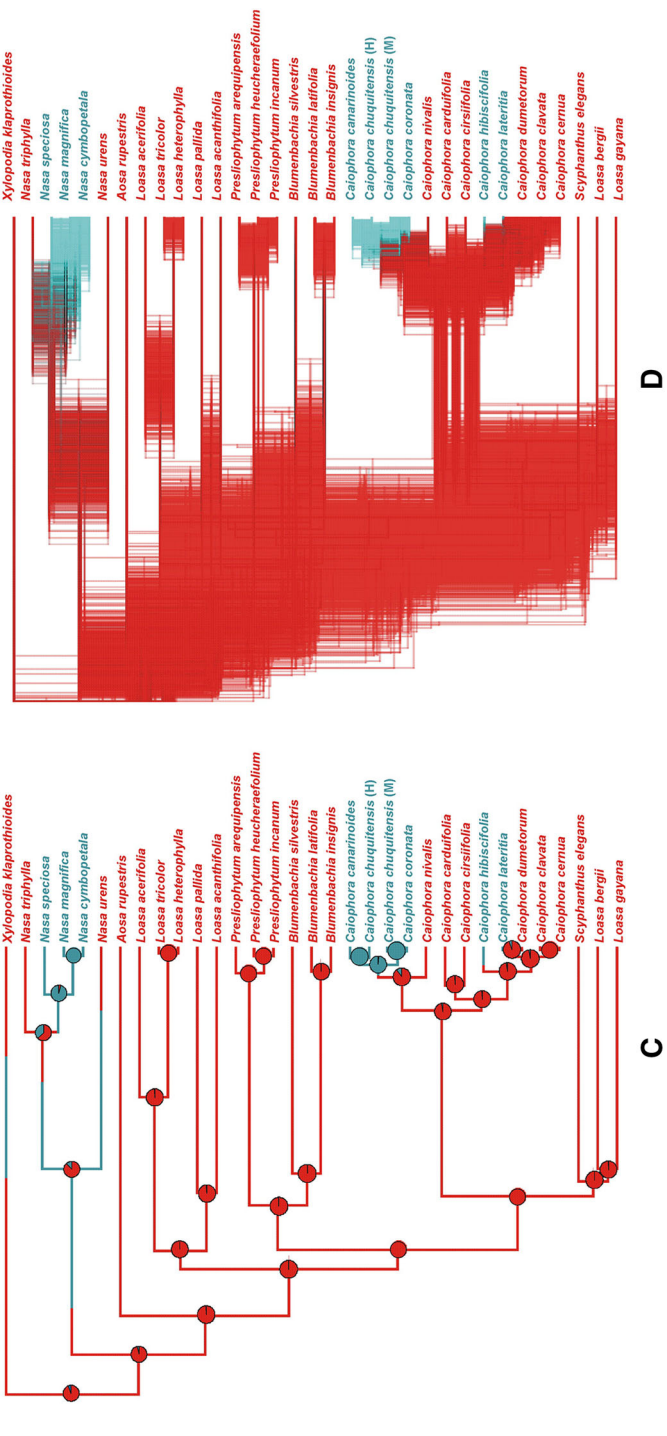

Fig. 2 continued

Table 1 Correlation state-by-state statistic d_{ij} and P values for tests of association between pollination modes and floral phenotypes

	d_{ij} value (P value)		
Flower type	Bee	Hummingbird	Small rodent
TRF	0.037 ($P < 0.0001$)	−0.0376 ($P < 0.0001$)	0.0003 ($P = 0.2$)
FRF	−0.037 ($P < 0.0001$)	0.0376 ($P < 0.0001$)	−0.0003 ($P = 0.2$)

The tests were performed with SIMMAP v 1.5 (Bollback 2006). Negative associations are indicated by a minus sign

The first PC obtained in the PCA analysis performed with the Procrustes coordinates of the corolla (PC_{1C}) and the staminodial complex (PC_{1SSt}) represented 90.58 and 69.51 % of variation in Procrustes coordinates, respectively. Since the PC_1 retrieved for each structure summarizes more than 50 % of shape variation, we did not use further PCs in the comparison of evolutionary models. For the corolla, PC_{1C} represents variation in the degree of corolla opening. Low values of PC_{1C} correspond to relatively closed corollas and high values correspond to extremely open corollas, with reflexed petals (Fig. 3c). For the staminodial

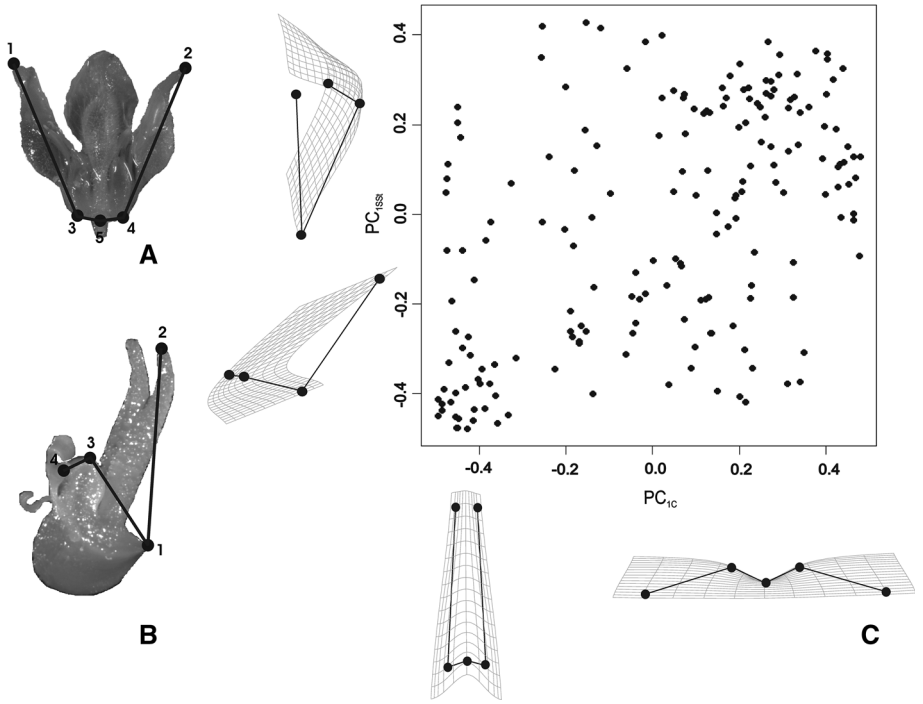

Fig. 3 Selected landmarks (**a**, **b**) and results of geometric-morphometric analyses (**c**). Photographs of the corolla (**a**) and the staminodial complex (**b**) in lateral view indicating the location of landmarks. **a** *Landmarks 1* and *2* are the upper extremes of the lateral petals; *landmarks 3* and *4* correspond to the position where the lateral petals are attached to the ovary; *landmark 5* corresponds to a point on the ovary in between the insertion of the lateral petals. **b** *Landmark 1* corresponds to the position where the nectar scale is attached to the ovary; *landmark 2* is the uppermost extreme of the staminode; *landmarks 3* and *4* are the right and left extremes of the opening on top of the nectar scale, respectively. The *solid lines* and the grids show the deformations of the consensus shape towards positive and negative values along each PC (**c**)

complex, PC_{1SSt} represents variation in the degree to which the staminodes protrudes from above the nectar scale neck and in the angle between the main axis of the nectar scale and the main axis of the staminodes (Fig. 3c). Low values of PC_{1SSt} correspond to staminodial complexes with the staminodes remarkably protruding from above the nectar scale neck and with the main axis of the nectar scale around 45° with respect to the main axis of the staminodes. High values of PC_{1SSt} correspond to staminodial complexes with the staminodes not remarkably protruding from above the nectar scale neck and with the main axis of the nectar scale almost oriented with the main axis of the staminodes.

According to the model comparison via AICc and the likelihood ratio test, PC_{1C} and PC_{1SSt} were under selection, as the BM model had always the worst fit (Table 2). PC_{1SSt}, model OU3 (OU with three adaptive optima corresponding to different pollination modes), attained the lowest AICc score and the best SIC score in the 1000 phylogenies sampled. PC_{1C}, model OU3, attained the lowest AICc score in 998 out of 1000 phylogenies, and the best SIC score in all phylogenies. In addition, the mean AICc value from model OU3 was significantly lower than the mean AICc value from the other models (in all cases Wilcoxon test $P < 0.0001$; supplementary material, Fig. S7), and similar results were obtained with SIC values (in all cases Wilcoxon test $P < 0.0001$; Fig. S7). According to the parameters from the best model (OU3), the optimum for hummingbird pollination was represented by a low PC_{1C} value, corresponding to a relatively closed corolla, and by a low PC_{1SSt} value, corresponding to remarkably protruding staminodes, flexed to ~45° with respect to the main axis of the nectar scale (Table 3; Fig. 4). The optimum for bee pollination was represented

Table 2 AICc and SIC values, ΔAICc and ΔSIC, degrees of freedom, log likelihood and *P* value of the likelihood ratio test between the selected model and the immediately related simpler model from each model comparison

Trait	Model	AICc	ΔAICc	SIC	ΔSIC	*df*	logLik	*P* logLik
PC_{1C}	BM	20.222		21.032		2	−7.683	
	OU 1	8.013	12.209	8.666	12.366	3	−0.083	0.0095
	OU 3	**4.735**	**3.278**	**3.447**	**5.219**	**5**	**5.360**	**0.0537**
PC_{1SSt}	BM	17.470		18.280		2	−6.306	
	OU 1	4.669	12.801	5.322	12.958	3	1.589	0.0075
	OU 3	**−5.407**	**10.076**	**−6.695**	**12.017**	**5**	**10.431**	**0.0036**

The model selected for each trait is in bold

Table 3 Values of the parameters from an OU model of trait evolution involving three adaptive optima (OU3)

Parameter	PC_{1C}	PC_{1SSt}
σ^2	2.943 (0.316–98.201)	0.521 (0.092–12.348)
α	45.025 (0.273–96.461)	11.678 (2.502–934.696)
θ_b	0.206 (0.093–0.321)	0.130 (0.032–0.241)
θ_h	−0.263 (−0.851 to −0.097)	−0.452 (−1.445 to −0.175)
θ_r	0.245 (−1.066 to 4.068)	2.781 (0.139–13.843)

σ^2, α and θ estimated for each trait along with their bootstrap confidence intervals encompassing the 2.5 % and the 97.5 % quantiles. θ_b, θ_h and θ_r are the optima for bee, hummingbird and rodent mediated pollination, respectively

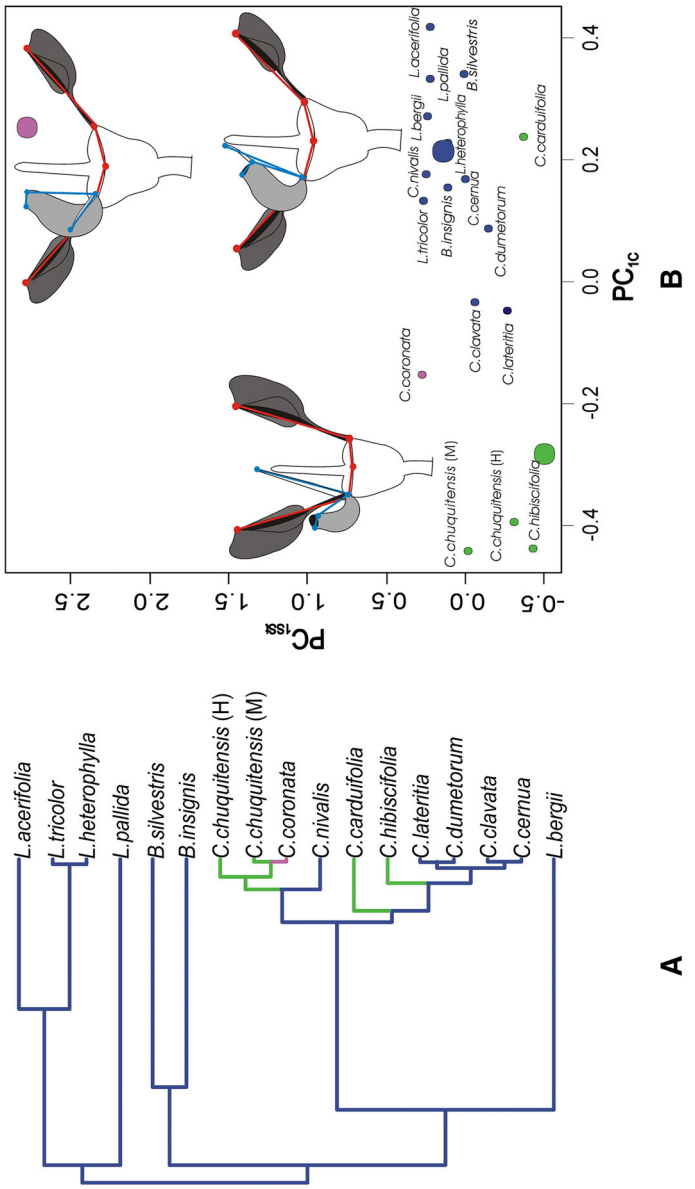

Fig. 4 Evolution of PC_{1C} and PC_{1SSt} in response to pollinator selection. Pollination strategies are indicated with different colours: *blue* = bee pollination; *green* = hummingbird pollination; *purple* = rodent pollination. **a** The pruned maximum credibility tree is shown with branches painted according to the reconstructed ancestral pollination strategy. **b** The optimal trait configurations for bee, hummingbird and rodent pollination in Loasoideae estimated for these variables are shown (*large circles*) along with the mean trait configurations of each analyzed species. The shape configurations corresponding to each optimum were added to the plot (the relative sizes of the corolla and the staminodial complex are not in the real scale). *Red* = landmark configuration of the corolla; *cyan* = landmark configuration of the staminodial complex. (Color figure online)

by a high PC_{1C} value, corresponding to an open corolla, and by a comparatively higher PC_{1SSt} value, corresponding to a staminode not remarkably protruding above the scale neck and with the main axis of the nectar scale almost aligned with the main axis of the staminode (Table 3; Fig. 4). The optimum for rodent pollination was represented by a high PC_{1C} value, corresponding to an open corolla, and by an extremely high PC_{1SSt} value (far beyond the values observed for *C. coronata*), corresponding to a staminodial complex with the staminode extremely reduced compared to the nectar scale (Table 3; Fig. 4).

Discussion

Our results suggest that flower shape can respond to pollinator selection during transitions from bee to bird pollination in a plant lineage lacking corolla tubes or nectar spurs. As suggested by Weigend and Gottschling (2006), and Ackermann and Weigend (2006), correlation between pollinators and flower phenotype is supported by the high proportion of overlap between the stochastic character mappings of pollinators and the TRF–FRF categorization, as well as by the test of evolutionary association between pollination mode and flower phenotype. Furthermore, when using geometric morphometric variables in alternative evolutionary models, we found that the evolution of the shape of the corolla and the staminodial complex is better described by an adaptive model with three optima corresponding to the three pollination modes in Loasoideae. Although hummingbird pollination is present in other plant lineages with radial flowers lacking tubes or spurs, e.g. *Passiflora*, (Kay 2001; Hansen et al. 2006) and *Malvaviscus*, (Webb 1984), this is the first macro-evolutionary study reporting flower shape modifications during the transition from bee to hummingbird pollination involving such floral design. In addition, we found evidence that staminodial structures in Loasoideae adapted their shape to hummingbird and even to rodent pollination, which may help to understand the role of these structures in other plant lineages.

The stochastic character mapping suggests four independent transitions from bee to hummingbird pollination, and one transition from hummingbird to rodent pollination in Loasoideae. Three of these transitions to hummingbird pollination also correspond to three independent changes in flower phenotype (Fig. 2). Interestingly, although hummingbird pollination is proposed to be the end-point in the evolution of pollination syndromes in several plant lineages (Barrett 2013 and literature therein, but see Whittall and Hodges 2007 and Tripp and Manos 2008), this seems not to be the case in Loasoideae, since the single rodent pollinated species (*C. coronata*) evolved in a subclade where hummingbird pollination is the prevailing condition. When Barrett (2013) proposes bird pollination to be the end-point in the evolution of pollination syndromes, he is considering lineages with tubular corollas, e.g. *Penstemon*, *Mimulus*, *Ipomoea*. Perhaps, the particular flower design of Loasoideae favours transitions from hummingbird pollination to other pollination syndromes, which may be limited in plant lineages with tubular corollas because of functional or structural constraints (Endress 2011). Interestingly, the South African genus *Protea* (Valente et al. 2009), presents transitions from bird to rodent pollination and, although flowers present corolla tubes, tubes are quite short, which can also be observed in bird pollinated species. Perhaps, the short corolla tubes, or eventually their complete absence, eased transitions from bird to rodent pollination in *Caiophora* and *Protea*. Reversals to bee pollination apparently did not take place in Loasoideae, suggesting strong directionality in transitions between pollination syndromes. This strong directionality is

also reported in other angiosperm lineages, e.g. *Aquilegia* (Whittall and Hodges 2007), and may be a consequence of the loss of ancestral developmental programmes and biosynthetic pathways (Barrett 2013). Indeed, there is preliminary evidence suggesting that the ancestral developmental program of the flower experienced remarkable modifications during the diversification of the genus *Caiophor*a (Strelin et al. in press). Nevertheless, the number of taxa in our study in not sufficient to make strong inferences regarding directionality in the evolution of pollination syndromes.

According to the best OU model, shape variables (principal components of Procrustes coordinates) evolved towards different adaptive optima, determined by bee, hummingbird and rodent pollination. The bee pollination optimum can be characterized by an open corolla and a staminodial complex with the staminodes almost aligned with the main axis of the nectar scale and slightly protruding from above its neck. The hummingbird pollination optimum in *Caiophora* can be characterized by a relatively closed corolla and a staminodial complex with staminodes remarkably protruding from above the nectar scale neck at a wide angle with respect to the main axis of the scale (this would make nectar at the bottom of the nectar scale more accessible to pollinators). These two optimal configurations conform to the TRF–FRF distinction, which supports the hypothesis that TRF and FRF are related to bee and hummingbird pollination, respectively (Weigend and Gottschling 2006; Ackermann and Weigend 2006). Since FRF in *Nasa* and *Caiophora* exhibit staminodial complexes with different architectures, it would be worth obtaining and incorporating to evolutionary modelling geometric morphometric variables describing the shape of this structure in hummingbird pollinated *Nasa* species. Differences in the shape of the staminodial complex between *Nasa* and *Caiophora* hummingbird-pollinated species may constitute a case of incomplete convergence (Losos 2011), similar to what happened in Rafflesiaceae, where complex flower morphologies evolved independently in response to fly pollination through distinctive developmental pathways (Nikolov et al. 2013).

Although Ackermann and Weigend (2006) assigned FRF to the single rodent pollinated species, *C. coronata*, the optimum for rodent pollination, characterized by an open corolla and extremely reduced staminodes, clearly differs from the optimum for hummingbird pollination. This may be explained first by the fact that no guiding function is accomplished by these structures in *C. coronata*, and second, by the fact that the licking foraging behaviour of rodents would be hampered by conspicuous staminodes. *C. coronata* has diverged recently from a presumably hummingbird pollinated ancestor (Fig. 2), which may explain why the PC_{1SSt} value observed in *C. coronata* is still far from the optimal staminodial shape for rodent pollination.

Summarizing our results, we postulate that flower shape responded to pollinator selection in Loasoideae, despite the flower design in this subfamily not including the corolla tubes or spurs, typical of plant lineages with transitions from bee to bird pollination syndrome. Perhaps, the staminodial complex was key to this transition, mediating flower–pollinator fit, and thereby enhancing the possibilities of specializing on different functional groups of pollinators. This may have not been possible if relying only on a corolla with distinct petals, not capable of properly filtering out less efficient pollinators (Thomson and Wilson 2008). Future studies accounting for the current efficiency of bee, hummingbird and rodent pollinators; and for how flower shape conditions this efficiency, would improve our understanding of how flower–pollinator interactions gave rise to flower shape diversity in Loasoideae.

Acknowledgments We thank Gabriela Gleiser, Lorena Ashworth, Romina Vidal Russell, Juan Fornoni, Marcelo Aizen and Mariano Ordano for contributing with their comments and suggestions to the quality of

this manuscript; to Maximilian Weigend for sharing his knowledge on the pollination mechanism of Loasaceae subfam. Loasoideae, the Botanical Gardens Bonn, Germany and Guillermo Amico for providing plant material and to Martin Diller, Alicia Sérsic, Jorge Strelin, Adrian Strelin, Leonardo Torielli and Salvador Marino for assisting in the field work. We also thank Laura Gatica for editing the English version of the manuscript and two anonymous reviewers for their comments on previous versions of the manuscript. Funds were provided by the Alexander von Humboldt Foundation (Germany), Fondo Nacional de Ciencia y Tecnología (FONCyT, Argentina, BID 2012 PID 1553), Consejo Nacional de Ciencia y Tecnología (CONICET, Argentina), Ministerio de Ciencia y Tecnología de la Provincia de Córdoba (MINCyT Grant 000113/2011 to AAC) and Secretaría de Ciencia y Tecnología of the Universidad Nacional de Córdoba (SECyT-UNC Grant 30820110100206 to SBV). M.S has a scholarship from CONICET.

References

Ackermann M, Weigend M (2006) Nectar, floral morphology and pollination syndrome in Loasaceae subfam. Loasoideae (Cornales). Ann Bot 98:503–514

Ashworth L, Aguilar R, Martén-Rodríguez S et al (2015) Pollination syndromes: a global pattern of convergent evolution driven by the most effective pollinator. In: Pontarotti P (ed) Evolutionary biology: biodiversification from genotype to phenotype. Springer, Marseille, pp 203–224

Barrett CHB (2013) The evolution of plant reproductive systems. How often are transitions irreversible? Proc R Soc Lond [Biol] 280(1765):20130913

Benitez-Vieyra SM, Fornoni J, Pérez-Alquicira J et al (2014) The evolution of signal-reward correlations in bee- and hummingbird-pollinated species of *Salvia*. Proc R Soc Lond [Biol] 281(1782):20132934

Bollback JP (2006) Simmap: stochastic character mapping of discrete traits on phylogenies. BMC Bioinform 7:88

Bouckaert R, Heled J, Kühnert D et al (2014) BEAST 2: a software platform for Bayesian evolutionary analysis. PLoS Comput Biol 10:e1003537. doi:10.1371/journal.pcbi.1003537

Brown DK, Kaul RB (1981) Floral structure and mechanism in Loasaceae. Am J Bot 68:361–372

Butler MA, King AA (2004) Phylogenetic comparative analysis: a modelling approach for adaptive evolution. Am Nat 164:683–695

Castellanos MC, Wilson P, Thomson JD (2004) "Anti-bee" and "pro-bird" changes during the evolution of hummingbird pollination in *Penstemon* flowers. J Evol Biol 17:876–885

Cocucci AA, Sérsic AN (1998) Evidence of rodent pollination in *Cajophora coronata* (Loasaceae). Plant Syst Evol 211:113–128

Endress PK (2011) Evolutionary diversification of the flowers in angiosperms. Am J Bot 98:370–396

Fenster CB, Armbruster WS, Wilson P et al (2004) Pollination syndrome and floral specialization. Annu Rev Ecol Evol Syst 25:375–403

Hansen TF (1997) Stabilizing selection and the comparative analysis of adaptation. Evolution 51:1341–1351

Hansen AK, Gilbert LE, Simpson BB et al (2006) Phylogenetic relationships and chromosome number evolution in *Passiflora*. Syst Bot 31:138–150

Harmon LJ, Weir JT, Brock CD et al (2008) GEIGER: investigating evolutionary radiations. Bioinformatics 24:129–131

Huelsenbeck JP, Nielsen R, Bollback JP (2003) Stochastic mapping of morphological characters. Syst Biol 52:131–158

Hufford L (2003) Homology and developmental transformation: models for the origins of the staminodes of Loasaceae subfamily Loasoideae. Int J Plant Sci 164:409–439

Hufford L (2005) A phylogenetic analysis of Loasaceae, subfamily Loasoideae based on plastid DNA sequences. Int J Plant Sci 166:289–300

Katoh K, Standley DM (2013) MAFFT multiple sequence alignment software version 7: improvements in performance and usability. Mol Biol Evol 30:772–780

Kay E (2001) Observations on the Pollination of *Passiflora penduliflora*. Biotropica 33:709–713

Klingenberg CP (2011) MorphoJ: an integrated software package for geometric morphometrics. Mol Ecol Res 11:353–357

Losos JB (2011) Convergence, adaptation and constraint. Evolution 65:1827–1840

Müller J, Müller K, Quandt D et al (2010) PhyDe—phylogenetic data editor. Program distributed by the author. http://www.phyde.de/index.html

Nielsen R (2002) Mapping mutations on phylogenies. Syst Biol 51:729–739

Nikolov LA, Endress PK, Sugumaran M et al (2013) Developmental origins of the world's largest flowers, Rafflesiaceae. Proc Natl Acad Sci 110:18578–18583
Revell LJ (2012) phytools: an R package for phylogenetic comparative biology (and other things). Methods Ecol Evol 3:217–223
Revell LJ (2014) Graphical methods for visualizing comparative data on phylogenies. In: Garamszegi LZ (ed) Modern phylogenetic comparative methods and their application in evolutionary biology. Springer, Heidelberg, pp 77–103
Rohlf FJ (2009) TPS series software. http://life.bio.sunysb.edu/ee/rohlf/software.html
Rosas-Guerrero V, Aguilar R, Martén-Rodríguez S et al (2014) A quantitative review of pollination syndromes: do floral traits predict effective pollinators? Ecol Lett 17:388–400
Strelin M, Benitez-Vieyra S, Fornoni J, Klingenberg CP, Cocucci AA (in press) Exploring the ontogenetic scaling hypothesis during the diversification of pollination syndromes in *Caiophora* (Loasaceae, subfam. Loasoideae). Ann Bot
Thomson JD, Wilson P (2008) Explaining evolutionary shifts between bee and hummingbird pollination: convergence, divergence and directionality. Int J Plant Sci 169:23–38
Tripp EA, Manos PS (2008) Is floral specialization an evolutionary dead-end? Pollination system transitions in *Ruellia* (Acanthaceae). Evolution 62:1712–1737
Valente LM, Reeves G, Schnitzler J et al (2009) Diversification of the African genus *Protea* (Proteaceae) in the Cape biodiversity hotspot and beyond: equal rates in different biomes. Evolution 64:745–760
van der Niet T, Johnson SD (2012) Phylogenetic evidence for pollinator driven diversification of angiosperms. Trends Ecol Evol 27:353–361
Venables WN, Ripley BD (2002) Modern applied statistics with S, 4th edn. Springer, New York. ISBN 0-387-95457-0
Webb CJ (1984) Hummingbird pollination of *Malvaviscus arboreus* in Costa Rica. NZ J Bot 22:575–581
Weigend M (2004) Four new species of *Nasa* ser. *Alatae* (Loasaceae) in the Amotape-Huancabamba zone of Peru. Novon 14:134–146
Weigend M, Gottschling M (2006) Evolution of funnel-revolver flowers and ornitophily in *Nasa* (Loasaceae). Plant Biol 8:120–142
Weigend M, Ackermann M, Henning T (2010) Reloading the revolver—male fitness as a simple explanation for complex reward partitioning in *Nasa macrothyrsa* (Loasaceae, Cornales). Bot J Linn Soc 100:124–131
Whittall JB, Hodges SA (2007) Pollinator shifts drive increasingly long nectar spurs in columbine flowers. Nature 447:706–709
Wilson P, Castellanos MC, Hogue JN, Thomson JD, Armbruster WS (2004) A multivariate search for pollination syndromes among penstemons. Oikos 104:345–361